RC columns strengthened by steel caging: cyclic loading tests on beam-column joints with non-ductile details

Joaquín G. Ruiz-Pinilla[a,*], Antoni Cladera[a], Francisco J. Pallarés[b], Pedro A. Calderón[b], Jose M. Adam[b]

[a]*Department of Industrial Engineering and Construction, University of the Balearic Islands, Palma, 07122, Spain. Tel.: +34 971 17 3000*

[b]*ICITECH, Universitat Politècnica de València, Valencia, 46022, Spain. Tel.: +34 96 387 7000*

Abstract

Beam-column joints suffer intense damage from seismic events and are the cause of many buildings collapsing. These zones present complex behaviour under cyclic loads, including tensile-compression cycles, which make reinforcement adherence worse and cause severe cracking in concrete. Although columns can be strengthened by various methods (e.g. concrete jacketing, fibre-reinforced polymers and steel jacketing-caging), beam column joints require complex systems being applied, but are not always effective. In Europe, fitting steel caging around columns is one of the most frequently used techniques, although its effectiveness against seismic events requires further study. The aim of this work is to analyse the behaviour of beam-column joints strengthened by steel caging subjected to cyclic loading, for which an ambitious experimental campaign was carried out on seven full-scale steel-caged specimens with a variety of strengthening solutions at joints. The results provide insight into the complex behaviour of joints with columns strengthened in this way, used as the basis for practical recommendations for engineers and architects who have to routinely retrofit structures against seismic events.

Keywords: Seismic strengthening; Retrofitting; RC beam-column joint; Steel caging; Cyclic loads; Experimental test.

1. Introduction

Earthquakes are still one leading cause of loss of human lives and structural damage [1,2]. In recent years, some of the most dramatic events include earthquakes in Iran, the Philippines, Pakistan and China in 2013, Indonesia and Iran in 2012, Japan and Turkey in 2011, Haiti and China in 2010, and Indonesia and Italy in 2009. According to a review by Doocy [3] on events between 1980 and 2009, during this period almost 400,000 people lost their lives, while around 61.5 million were seriously affected by earthquakes.

Many studies have been published on the damage caused by earthquakes to reinforced concrete structures that evidence severe damage to columns and joints, including events in: Lorca, Spain in 2011 [4]; Van, Turkey in 2011 [5–8]; Bingöl, Turkey in 2003 [9]; Hyogo-ken Nanbu, Japan in 1995 [10]; L'Aquila, Italy in 2009 [11]; various earthquakes in Turkey [12], among others. Other studies have highlighted the negative effect of marine environments on the behaviour of concrete structures close to coasts in seismic movements [13,14], which may also need interventions to improve their seismic response. Chloride corrosion causes general building stiffness loss and local reduction of ductility in columns [13].

The most frequently used types of column strengthening [15] include reinforced concrete jacketing [16–18], externally bonded fibre-reinforced polymer jacketing [19–21] and steel jacketing [22–26]. Other possible hybrid [27] and shape memory alloy types [28] have also been studied. Although all these techniques are based on confining columns to increase their axial, shear and bending strengths, not only beams and columns should be taken into account when computing a building's seismic strength, but the fact that horizontal loads against which beam-column joints play a crucial role should also be remembered. These can fail either before or after the yielding of the beam or column reinforcement [29]. Cracked joints have serious implications in structural analyses [30], especially in buildings designed to resist only vertical loads given the brittle nature of joint failures [31]. The strength of a structure with strengthened columns could, therefore, be restricted by joints' strength and ductility.

Joints are responsible for transmitting loads between columns and beams in a very small area that has to withstand high concentrations of compression and shear loads [32], while the reinforcement that passes through joints is subjected to tensile and compression cycles that affect their adherence and can damage the surrounding concrete [33]. Under gravity loads, the top reinforcement layer in beams is subjected to tensile loads, while their lowest layer of concrete is under compression, so that the design of the beam reinforcement is not usually either symmetrical or continuous. Under horizontal loads, original tensile and compression loads begin to oscillate. For all these reasons, joints' behaviour and the loads that act on them depend on the combination of gravitational and horizontal loads and the arrangement of its internal reinforcement.

Strengthening joints is somewhat more complicated than strengthening columns because they are usually placed within slabs and there may be other nearby damage-prone elements. Several studies on strengthening beam-column joints [34] have been published, some by increasing the joint panel size [35,36], others by using fibre polymer reinforcement [37–41] and several by employing external steel elements [42–44].

This paper describes an ambitious experimental campaign on full-scale beam-column joints with columns strengthened by steel caging. The aim was to study the cyclic behaviour of different contact configurations between strengthening and joints to design a technique that strengthens existing structures that were designed to withstand only gravity loads and are, thus, susceptible to damage by seismic events.

The results led to an easy-to-apply strengthening solution for existing structures without having to open the joint panel, in which the column is strengthened by longitudinal angled corner-pieces and battens, and joints are strengthened by steel capitals welded to the column jacket. The full-scale tests on this joint type posed a considerable challenge and had to be done in two consecutive and coordinated stages given the simultaneous application of gravity loads and horizontal loads on beams and columns. The proposed strengthening technique improved internal reinforcement adherence, the ability of beams to reverse moments and the beneficial effect of strengthening on the beam-column joint's cyclic behaviour.

2. Experimental program

The experimental program was designed to study the behaviour of steel caging as a column strengthening system for the typical buildings designed in the 1980s and 1990s in southern Europe, and other parts of the world, to withstand only gravity loads, and which lack the necessary ductility to resist the horizontal actions endemic to seismic movements.

2.1 Design of specimens

Five beam-column joint types were studied, some in duplicate to verify the results, with a total of seven specimens. A specimen with a non-strengthened joint (*A.W.L0*) was used as the reference. A summary of the specimen characteristics can be seen in Table 1.

The first letter *A* of the specimen nomenclature refers to the type of beam reinforcement: *Asymmetric* means different upper and lower reinforcement types. The next letter indicates the joint strengthening type: *W*, not strengthened; *C*, capital only; *CA*, capital plus chemical anchor. The next is the axial load level applied to columns: *L0*, normalised axial ν = 0; *L1*, normalised axial ν = 0.3.

Table 1. Number and characteristics of the tested specimens.

Nº	Specimen	f_c [MPa]	Joint strengthening	Axial load ($N=\nu \cdot A_c \cdot f_c$) [kN]
1	A.W.L0	23.2	--	0
2	A.C.L0	20.7	Capital	0
3	A.C.L1	23.2	Capital	625
4	A.CA.L0-1	15.6	Capital + chemical anchor	0
5	A.CA.L0-2	23.9	Capital + chemical anchor	0
6	A.CA.L1-1	13.2	Capital + chemical anchor	350
7	A.CA.L1-2	19.7	Capital + chemical anchor	530

Figure 1 provides the specimen dimensions. The 2,200 mm-long specimens consisted of 900 mm-long columns with a 300x300 mm cross-section, while beams measured 3,300 mm from end to end with a 300x400 mm cross-section and a length of 1,500 mm, as in other similar studies [45–47].

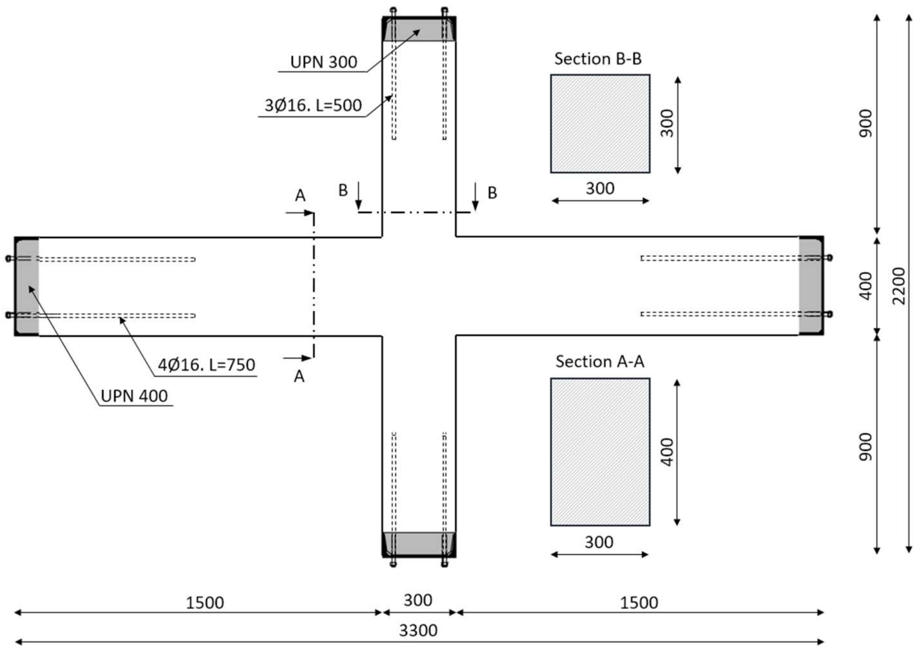

Figure 1. Specimen geometry (dimensions in mm).

The distance between inflection points was 2,800 mm in columns and 4,000 mm in beams, including the elements required to fix the specimen to the test frame, which were UPN steel pieces with welded plates. To ensure load continuity between the test frame and specimen, Ø16 mm corrugated bars were embedded in the beam and column ends.

The quality of the employed materials was similar to that used in typical buildings in the 1980s and 1990s. The mean compressive strength obtained from testing cylindrical specimens (on the same day as the test run on the corresponding specimen) was between 13.2 and 23.9 MPa (Table 1). B500SD steel was used with a yielding strength and ultimate strength of 550/660 MPa for Ø12 mm reinforcement and 570/675 MPa for Ø16 mm, respectively.

Beam reinforcement was asymmetric with different upper and lower quantities (see Figure 2). Two independent beam segments were used, which overlapped at the joint at 250 mm. Each segment had an upper longitudinal reinforcement of 2Ø12 and a lower one of 2Ø16 in the corners, with an additional upper reinforcement of 3Ø16 mm crossing the joint continuously to carry negative (hogging) bending moments. The transverse beam reinforcement was Ø8/100 mm. Other authors have used similar schemes [46–48].

The minimum amount of reinforcement was used in columns: 4Ø12 mm longitudinal reinforcement in each corner and Ø6/150 mm stirrups. The 4Ø12 mm longitudinal reinforcement was continuous with no overlaps to reduce the number of variables considered in the experimental program.

In order to avoid any possible problems caused by the concentration of loads due to local loads applied by actuators, the transverse reinforcement was increased at the ends of beams and columns (Figure 2).

No transverse reinforcement was placed inside the joint core in any specimen. The concrete cover was 25 mm in all the segments.

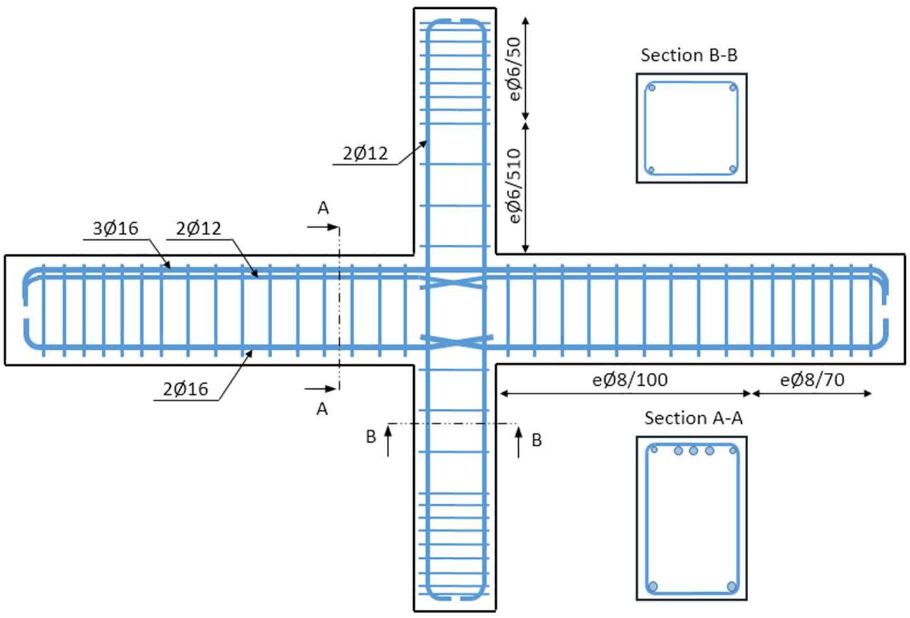

Figure 2. Reinforcement (dimensions in mm).

2.2 Strengthening technique

The strengthening technique consisted of placing vertical steel angle pieces in the corners of the columns welded to rectangular transverse steel battens after considering the results obtained in previous studies carried out at the ICITECH of the *Universitat Politècnica de València* [22,49–51].

S275 steel was used in strengthening (yielding strength 275 MPa). The steel elements remained in contact with the column surface by a cement mortar (1/2 cement/sand ratio).

The four corner angle pieces of the column were L70.7 mm and battens were 260x120x8 mm, except for those nearest the joint, where battens were larger, 280x160x8 mm (Figure 3). Angle pieces were welded at the ends to the UPN steel pieces to ensure the correct compatibility of the deformations at that point.

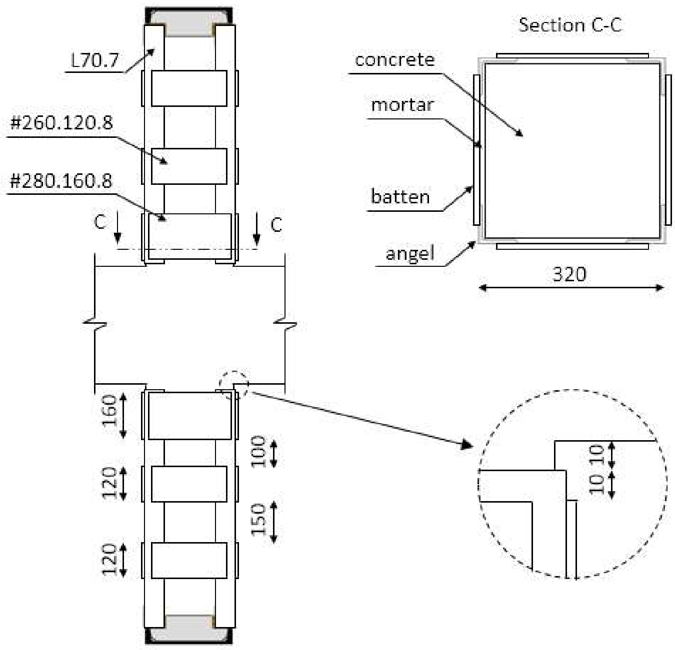

Figure 3. Steel caging (dimensions in mm).

Three types of column-joint connections were studied (Figure 4): one had no column-joint connection, while a steel angle (capital) was welded to the column strengthening in the other two that came into direct contact with the beam's surface. The difference between the last two types was that one had no joint-capital connection and the other used two Ø16 mm chemical anchors in each capital, which entered at a depth of 125 mm in concrete.

The capital was made with a larger section than that used for the columns, L100.14 mm, stiffened with 12 mm steel plates to reduce its deformability. Capital dimensions were based on the results of a previous study [50]. This capital was joined lengthwise to the metal battens and to the corner angle pieces at each end so that capitals were welded to the strengthening on three sides.

a. W typology. No connection. b. C typology. Capital. c. CA typology. Capital and chemical anchor.

Figure 4. Joint strengthening.

2.3 Test setup

Two types of actions were considered in the experiments: gravitational and horizontal. For the gravity load on the column, two normalised axial load values were fixed: 0 and 0.3. Both values represent the actions performed on the top and ground floors, respectively. The value of the load on beams was set at 30 kN and applied to the end of each beam to simulate slab loads (Figure 5a). This value was determined in such a way that the bending moment generated at the joint came close to that which would be generated at the same point in a structure of continuous beams under gravity loads acting on a slab during a seismic event, by considering the combination coefficients of actions in accidental situations. Authors such as [38,52,53] have also considered gravity loads on beams in their tests. Horizontal actions were applied by gradually incrementing cyclic loads until specimen failure in accordance with the scheme shown in Figure 5b.

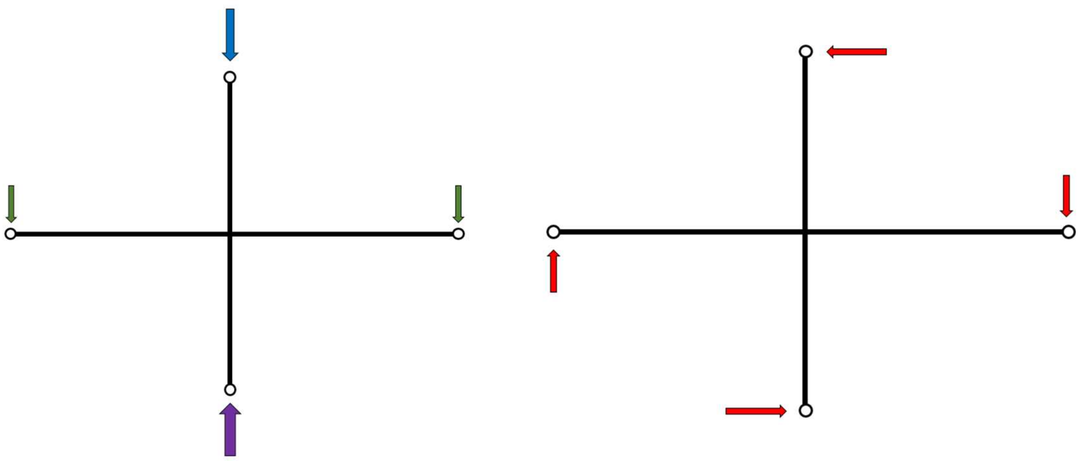

a. Gravity loads. b. Horizontal loads.

Figure 5. Loads applied to specimens.

According to the literature, two different techniques are used to apply horizontal actions [54]: one consists of applying them to the top of the column to allow beams to move horizontally, and not vertically (CL method) [53–55]; the other involves applying opposite vertical loads to the ends of beams to avoid the horizontal movement of column ends (BL method) [39,47]. This requires coordination between both hydraulic actuators, but completely controls the applied loads and the movement of beams, which is fundamental to correctly coordinate gravity and cyclical loads.

The test was carried out by the BL method in two phases: in the first one, the gravity load on beams was controlled by force control. In the second phase, this was controlled by moving beams. Thanks to this combination of phases, the gravity load on beams remained constant throughout the first phase and the first cycles of the second phase, in which the algebraic sum of loads on beams equalled the sum of the gravity loads on beams.

In the second phase, as movements increased and non-linear effects began to be noted, the algebraic sum gradually declined with the degradation of beam stiffness. The non-symmetry of beam reinforcement meant that the load they could stand differed according to the direction in which it was applied, which was the same case as that involved in the redistribution of loads in a concrete framed building.

Each cycle was repeated 3 times to detect whether or not degradation increased with each repetition, as in [56,57]. In the first phase, the loading rate was 0.33 kN/s at opposite beam ends until drift ratio values of 0.25%, 0.50% 0.75% and 1.00% were obtained. In the second phase, control was achieved by imposing displacement with a 120-second period per cycle and with a raising drift ratio of 0.50% until specimen failure occurred (Figure 6).

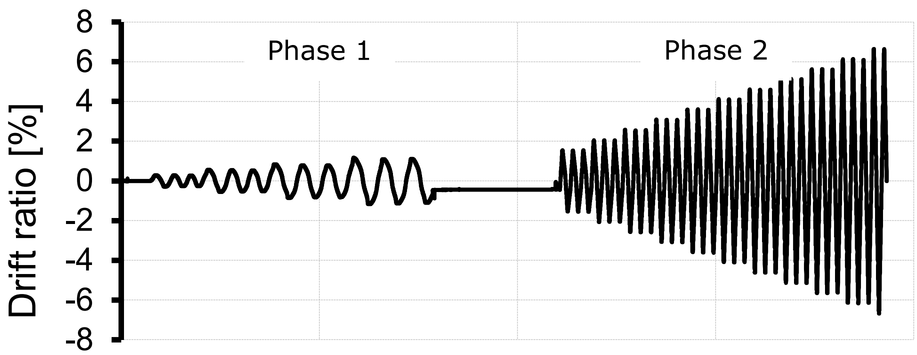

Figure 6. Load cycles (drift ratio & time).

All the test frame/specimen connections were hinged to rotate freely on the test plane. Figure 7 depicts a specimen ready for testing. Axial load was applied to the column by a 1000 kN hydraulic actuator. As the specimen was connected to the test frame at the point where the axial load was applied, the upper column end moved vertically, but not horizontally. Cyclic loads were applied to both ends of beams by two double-acting actuators with 250 kN load capacity and a displacement range of 500 mm.

Figure 7. Specimen in the test frame ready for testing.

The load protocol was as follows:

1. Constant axial load on column (L1 specimens only). Force control
2. Gravity load applied to beam ends. Force control.
3. Cyclic loads, first phase. Equal load increments applied to each beam in opposite directions. Force control.
4. Phase change. Recording the movements obtained in last cycle of the first phase to calculate the movements to be applied in the second phase. Displacement control.
5. Cyclic loads, second phase. Increased beam displacement until specimen loses at least 15% of its maximum strength.

2.4 Test monitoring system

Specimens were instrumented by strain gauges (Figure 8). The main objective of monitoring reinforcement was to study reinforcement adherence at joints, as in previous studies [46,58]. All the rebars in columns (*C1*-*C4*) were monitored in the two segments where the column met the joint (positions 1 and -1). Two opposite rebars (*C2* and *C3*) were also monitored in three more positions (positions -2, 0 and 2). Each column reinforcement was fitted with 14 strain gauges.

All the beam rebars (*BA1*-*BA4* and *BAC*) were monitored in the two segments where the beam met the joint (positions -2 and 2). The upper central reinforcement (*BAC*) and those at opposite corners (*BA1, BA4*) were monitored at six more points (positions -3, -1, 0, 0, 1, 3). Position 0 was repeated to measure the strain of both overlapping reinforcements at this point. Each beam had 27 strain gauges.

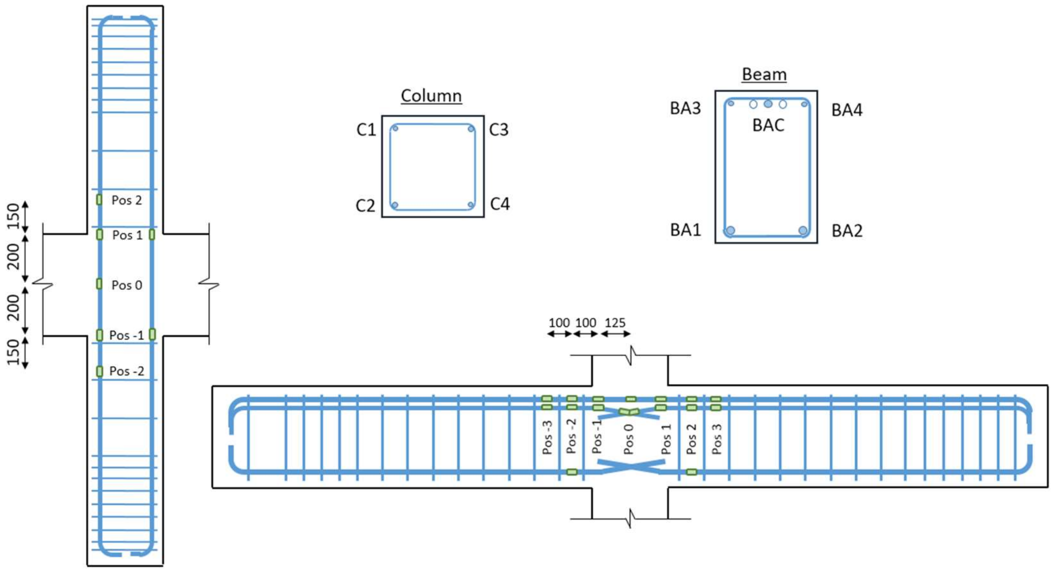

Figure 8. Monitoring internal reinforcement.

The steel-caging instrumentation is shown in Figure 9. A strain gauge was placed on each angle piece in the section closest to the joint between two battens (*S1*-*S4* in the upper segment, and *I1*-*I4* in the lower one, at a distance of 230 mm from the column base).

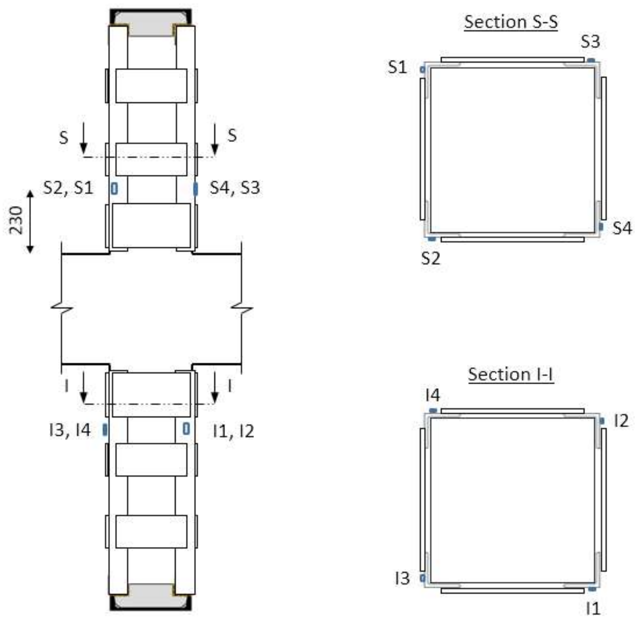

Figure 9. Steel-caging instrumentation.

3. Experimental results and discussion

3.1 Hysteretic response and failure modes

The obtained results are shown in Figure 10 by means of column shear load, *Vc*, in relation to relative displacement (drift), together with an image of the state of the beam-column joint in the first cycle for a given displacement value: +3.5% drift ratio for the tests with no axial load on columns, and +2.5% drift ratio for those with axial load.

Figure 10 shows two different types of cracking: bending cracks where the column meets the joint, negative (hogging) bending moment cracks in beams, positive (sagging) bending moment cracks in beams, and shear and compression cracks in the joint.

The effects of axial loads on columns can be seen in the graphs in the form of hysteresis loops. With no gravity loads on the column, marked pinching appeared (Figure 10a, Figure 10b and Figure 10c). Degradation occurred when the concrete lost part of its compressive strength in the beam and column segments due to joint shear deformation [59], plus loss of reinforcement adherence. The hysteresis loops obtained in the tests with the applied axial loads to columns clearly differed (Figure 10d and 10e).

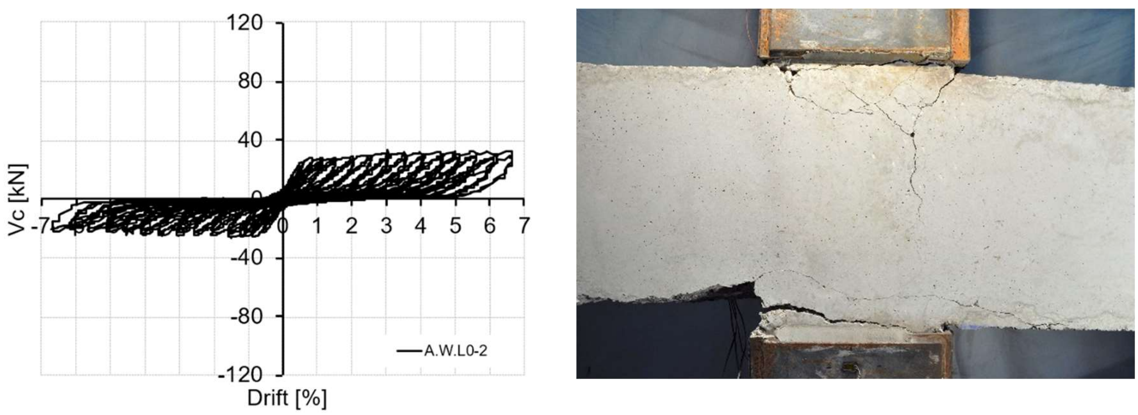

a. A.W.L0

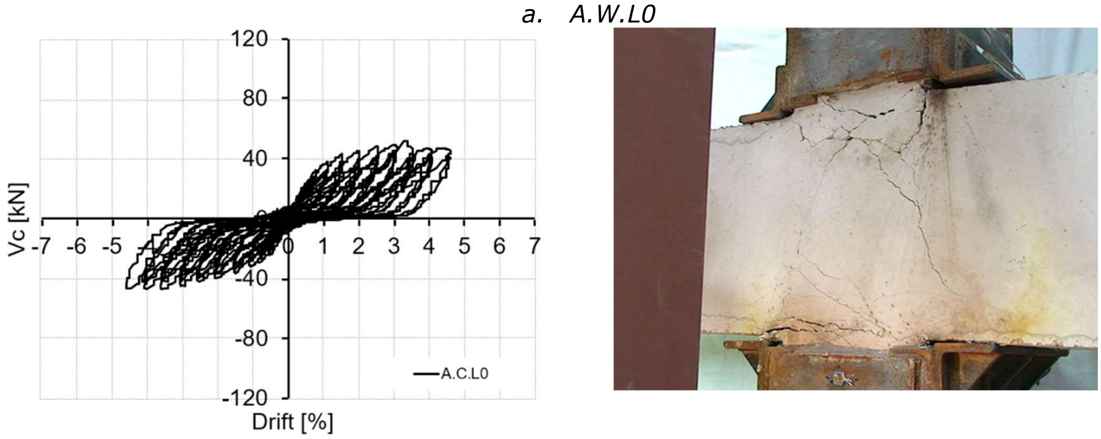

b. A.C.L0

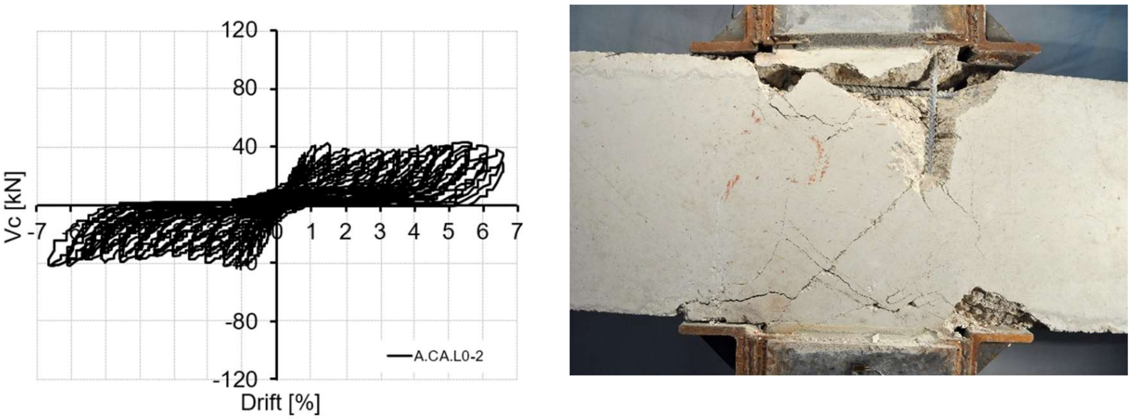

c. A.CA.L0-2

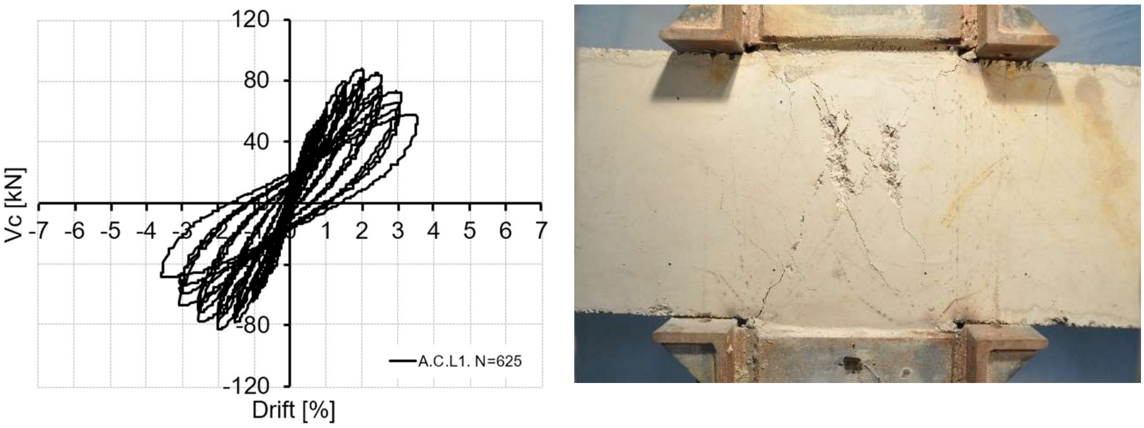

d. A.C.L1

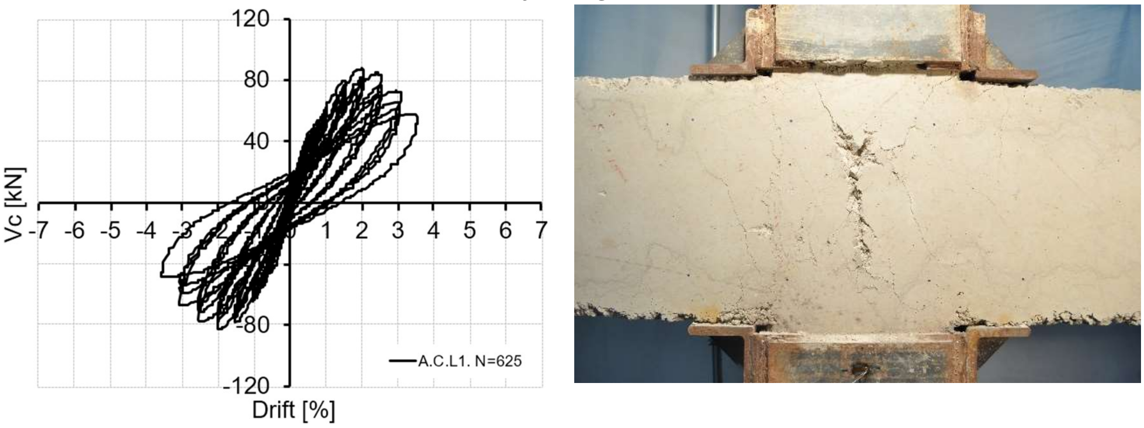

e. A.CA.L1-2

Figure 10. Left: column shear load vs. drift ratio. Right: joint view at the 3.5% drift ratio in the specimens with no axial loads on the column (L0), and a 2.5% drift ratio in those with axial load (L1).

Error! Not a valid bookmark self-reference. summarises the general results obtained in the tests: maximum shear load reached in specimens in both loading directions (V_c^+, V_c^-), the drift ratio for max shear in each movement direction ($Drift^+$, $Drift^-$), the mean value of both shear loads (V_{cm}) and the drift ratio value for 15% loss of max strength ($Drift_{85\%}$).

Table 2. General test results.

Specimen	**V_c^+ [kN]**	**V_c^- [kN]**	**$Drift^+$ [%]**	**$Drift^-$ [%]**	**V_{cm} [kN]**	**$Drift_{85\%}$ [%]**
A.W.L0	32.7	-25.9	5.5	-1.5	29.3	>5.0
A.C.L0	49.9	-46.9	3.0	-4.0	48.4	>4.5
A.C.L1	86.7	-82.8	2.0	-2.0	84.8	2.9
A.CA.L0-1	49.9	-41.4	2.5	-3.5	45.7	3.9
A.CA.L0-2	43.1	-42.1	1.5	-1.5	42.6	>6.0
A.CA.L1-1	68.7	-64.4	2.0	-2.0	66.6	2.3
A.CA.L1-2	77.8	-78.2	2.0	-2.0	78.0	2.9

The column shear value is not completely symmetrical in the positive and negative load directions (Table 1 and Figure 12a), due apparently to the position of the overlapping reinforcements inside the joint (Figure 11). As the corner reinforcement in beams overlapped inside the joint, a decision was made to overlap each pair of bars on the same plane (beside each other) by strictly following the same arrangement. On the left beam in Figure 11, the upper overlapping reinforcement (2Ø12) was placed outside that of those of the right beam, while the left beam lower reinforcements (2Ø16) were placed inside those of the right beam. In this way, for $Drift^+$ displacements the reinforcements of the beams under tensile loads were covered by most concrete and had, therefore, the most anchorage capacity. For $Drift^-$ displacements, the reinforcements of the beams under tensile loads had the least coverage and, thus, less anchorage capacity.

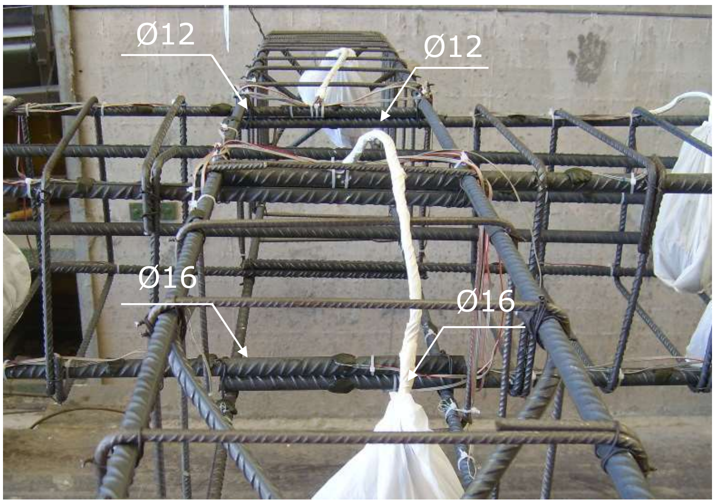

Figure 11. Arrangement of the overlapping reinforcements inside the joint.

Figure 12a shows the hysteretic curve envelopes of all the specimens. The control specimen (*A.W.L0*) maintained the load with great ductility when max. strength was limited by column reinforcement yielding. Figure 13a shows the separation between the column and joint elements.

The use of capitals (*A.C.L0*) increased strength by 65% compared to the control specimen, thanks to the larger supporting base of the column on the joint that they provided. This specimen with capitals also offered good ductility and reached a 4.5% drift ratio with no loss of strength, but the test was interrupted by an accidental power outage and no further data are available.

The use of chemical anchors did not improve specimens' cyclic behaviour, and even had a negative effect. The loads reached in *A.CA.L0-1* and *A.CA.L0-2* were 6% and 12% less than those in the test with no chemical anchors (*A.C.L0*), respectively. When the chemical anchor was subjected to tension loads, the concrete around it became damaged (Figure 13d). When the load direction was reversed, the already degraded concrete zone had to resist the compression transmitted by the capital with its lower capacity.

The specimens with axial loads (*A.C.L1, A.CA.L1-1* and *A.CA.L1-2*) reached the highest strength, but displayed more brittle behaviour as failure was governed by combined normal and bending loads. Figure 13e shows the buckling of the column reinforcement inside the joint. The load reached by specimens depended on the axial load value applied to the column.

Figure 12b indicates the shear load at each end of beams: *V1*, load of the left-hand actuator; *V2*, load of the right-hand actuator. Note that for the 0% drift ratio, the load on beams was 30 kN, which represents the initial gravity load applied at the beginning of the test.

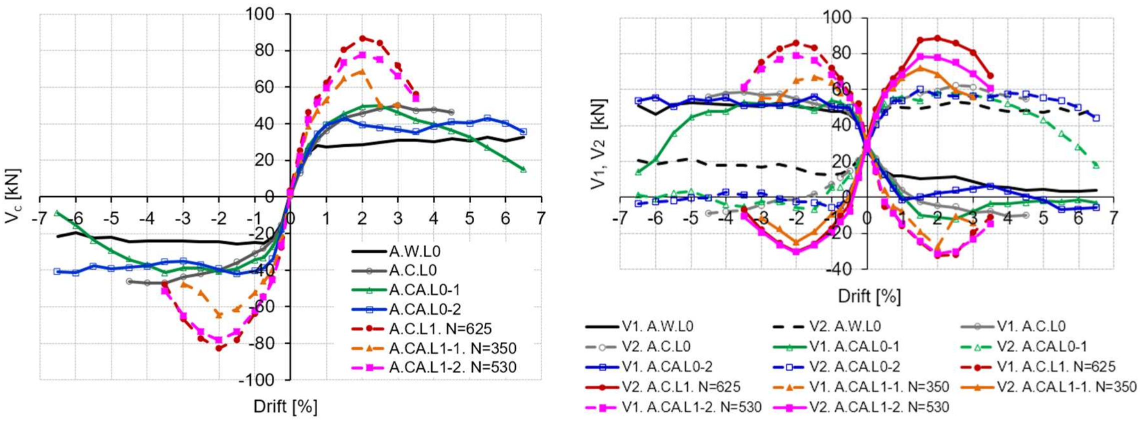

a. Shear load in column vs. drift. *b. Shear load in beams vs. drift.*

Figure 12. Envelope loads vs. displacement.

The specimens with no axial load (*A.W.L0, A.C.L0, A.CA.L0-1* and *A.CA.L0-2*) reached a similar maximum load in both beams in the gravity direction (positive value). This load was limited to beams' bending moment capacity due to the yielding of the 3Ø16 continuous rebars across the joint (Figure 2). The overlapping discontinuous reinforcements (both upper and lower) were not effective due to the large bending crack between the column and the joint: reinforcement did not remain in contact with concrete (Figure 13a, Figure 13b and Figure 13c). This separation removed the necessary reinforcement confinement for the overlapping reinforcements to be able to transmit loads due to the cyclic nature of the tests [33]. Beams could not withstand the inversion of bending moments. This effect is seen in Figure 12b, where no negative shear load values are applied to beams. In the tests with axial loads, greater loads were reached on beams in both the positive and negative gravity directions, which shows that axial load benefits the overlapping capacity of the discontinuous reinforcements inside the joint.

a. Crack between column and joint. A.W.L0

b. Loss of adherence. CA.L0-2

c. Capital separation. A.C.L0

d. Concrete damage beneath capital. A.CA.L0-1

e. Buckled column reinforcement. A.C.L1

Figure 13. Local damage observed during tests.

3.2 Energy dissipation capacity and stiffness degradation

Figure 14a shows the results of the energy dissipated in tests. The specimen without capitals dissipated the least energy, while the others had similar values in small displacements and with considerable differences in the larger ones. The specimens with axial loads on columns dissipated more energy for the same displacement, but failed earlier.

Figure 14b shows the stiffness obtained in tests. The reference specimen was by far the least stiff. Using capitals increased column stiffness, and did so further with an axial load on the column. However, stiffness degraded rapidly in all cases with 50% loss for the 1.5% drift ratio.

It should be noted that the stiffness of the specimen with capital (*A.C.C0*) was initially similar to the reference specimen (*A.W.L0*) and it was finally equal to both specimens with capital and chemical anchors. This was due to all the capitals not having without mortar and coming into direct contact with the beam. In the specimens with chemical anchors, the used resin partially filled the small space between the capital and beam so that the specimen with capitals was only less stiff initially until the capital came into contact with the beam's surface due to column bending deformation.

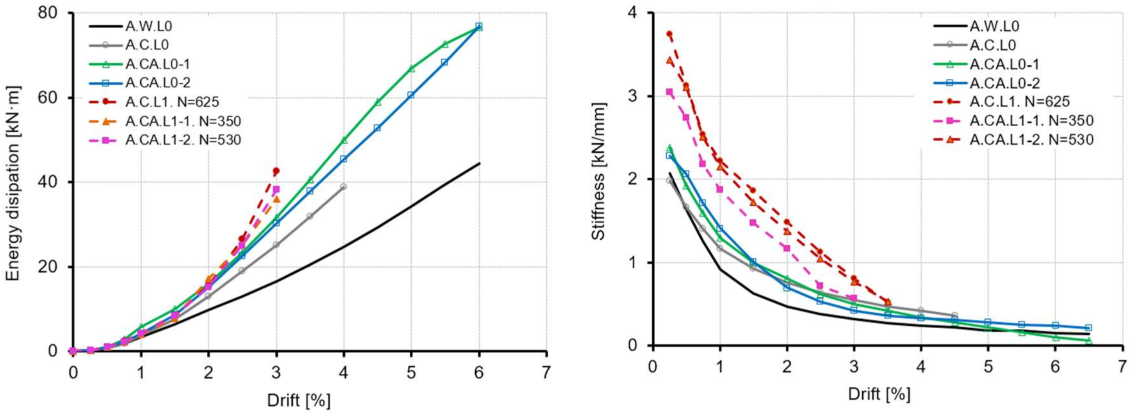

Figure 14. Energy dissipation and stiffness degradation.

3.3 Reinforcement behaviour

This section presents the main obtained results, including: reinforcement strain at various points (see Figure 8); adherence conditions inside the joint; effectiveness of the discontinuous overlapping reinforcements; the effect of an axial load applied to the column. The reliability of the data obtained from strain gauges was verified by comparing the results of the symmetrically placed gauges.

Figure 15 illustrates the upper strain in *BAC* and *BA4* in tests *A.C.L0 and A.CA.L1-1*. The *X*-axis represents the distance in metres from the measurement point to the column axis (Figure 8); the *Y*-axis represents the strain recorded by the strain gauge under gravity loads only (Figure 5a), i.e. after three load cycles at each drift ratio (Figure 5b, Figure 6). The following reinforcement behaviour patterns were noted:

- When gravity load was applied to beams, the reinforcement strain at the mid-point of the joint was less than at the points where the beam entered the joint.
- After the first three cycles at the 0.25% drift ratio, the strains at all points into the joint (*Pos -1, Pos 0* and *Pos 1*) in the *BAC* reinforcement were equal, which indicates loss of adherence to the joint concrete and that reinforcement acted as a tie.

- Strain in the BA4 reinforcements gradually decreased after each cycle until a zero strain, which indicates complete loss of overlap.
- Figure 15d shows that the axial load on the column favoured the overlap effectiveness of discontinuous reinforcements.

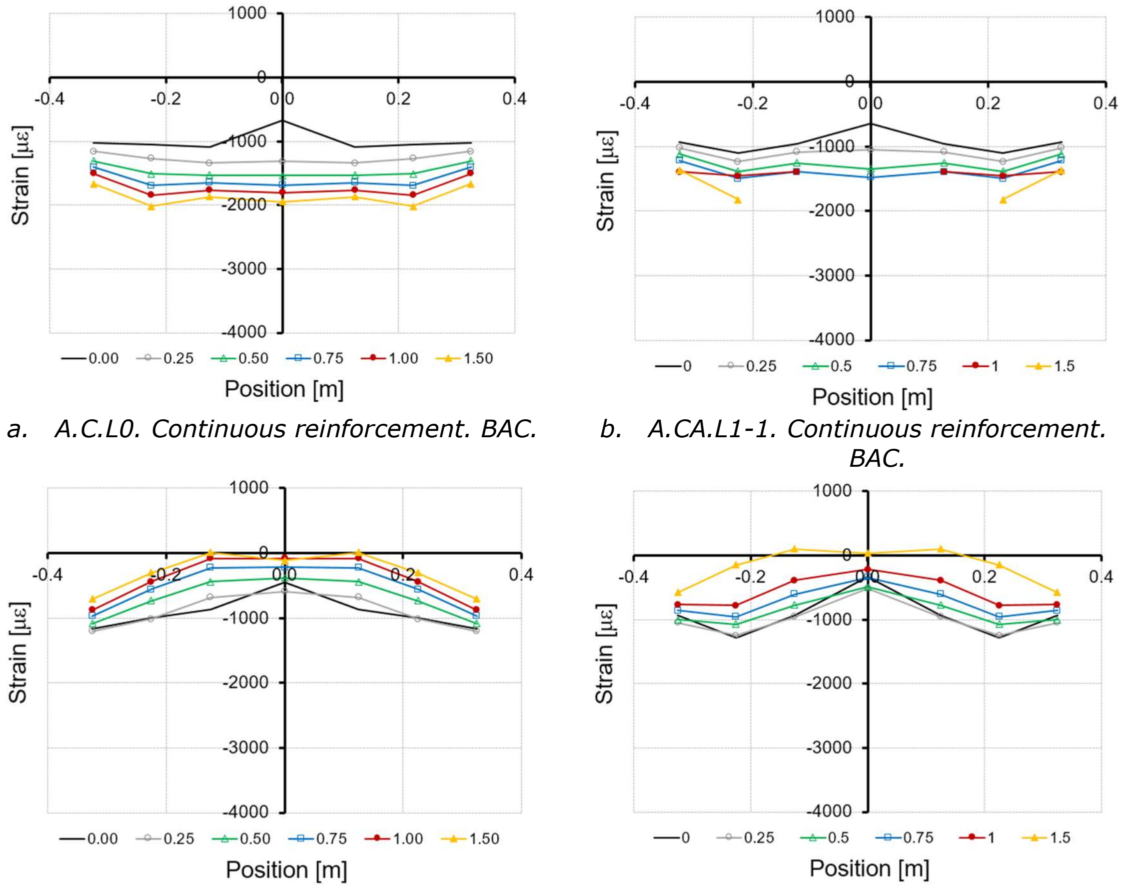

a. A.C.L0. Continuous reinforcement. BAC.

b. A.CA.L1-1. Continuous reinforcement. BAC.

c. A.C.L0. Discontinuous reinforcement. BA4.

d. A.CA.L1-1. Discontinuous reinforcement. BA4.

Figure 15. Strain of all the drift ratio values of the upper reinforcement in the beams of specimens A.C.L0 (left) and A.CA.L1-1 (right). Gravity load.

Figure 16 depicts the analysis of the reinforcement strain in the similar beam to that shown in Figure 15 but, in this case, the strain at each point was that recorded in the first cycle of each drift ratio value. The following observations were made:

- In Figure 16a, the tensile strain in the *BAC* upper reinforcement was constant up to approximately the column axis, after which it gradually declined due to adherence. It should be noted that this reinforcement was anchored to the other side of the joint, where concrete was compressed due to inverse beam moments (Figure 12b). In the specimen with the axial load (*A.CA.L1-1*), the *BAC* reinforcement anchorage was seen to start at the point where it entered the joint zone (Figure 16b).

- Although the continuity of tensile loads was not possible in discontinuous reinforcements *BA4* (Figure 15c and Figure 15d), certain reinforcement anchorage capacity was noted when the horizontal loads were applied (Figure 16c). The transmission of tangential stress between reinforcement and concrete in the joint was once again favoured by applying the axial load to the column (Figure 16d).
- Lower beam reinforcement *BA1* remained under compression strain at all the recording points in specimen *A.C.L0* (Figure 16e). The reinforcement compression strain can be seen on the right of the graph due to the negative bending moment, while there is no tensile strain on the left in spite of the reversed direction of loads. However, the lower reinforcement had greater anchorage capacity in the specimen with an axial load on the column (Figure 16f), thanks to which beams were able to reverse bending moments (Figure 12b).

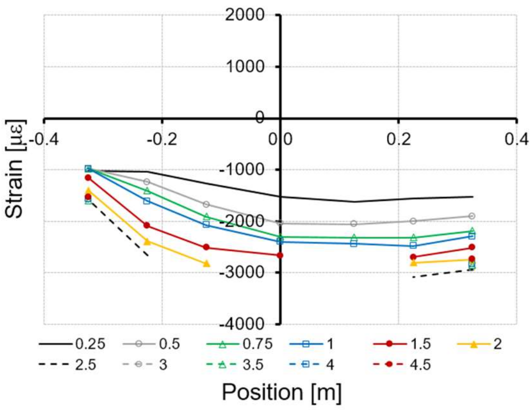

a. A.C.L0. Continuous reinforcement. BAC.

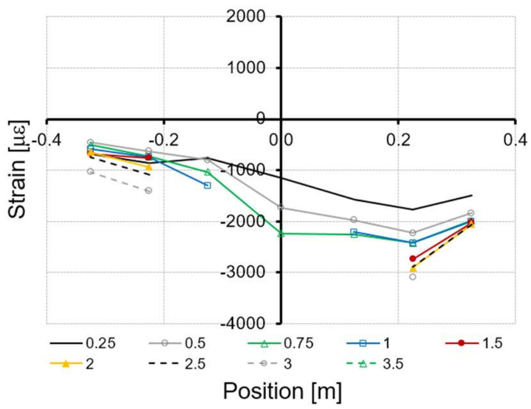

b. A.CA.L1-1. Continuous reinforcement. BAC.

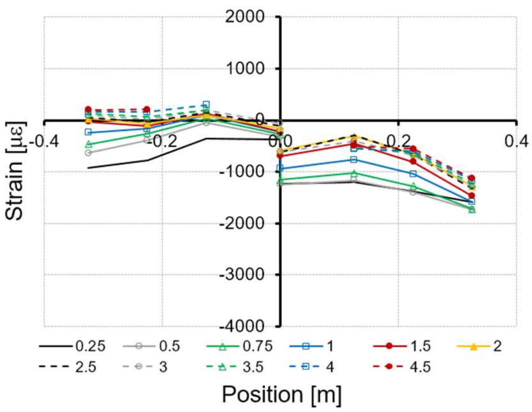

c. A.C.L0. Discontinuous reinforcement. BA4.

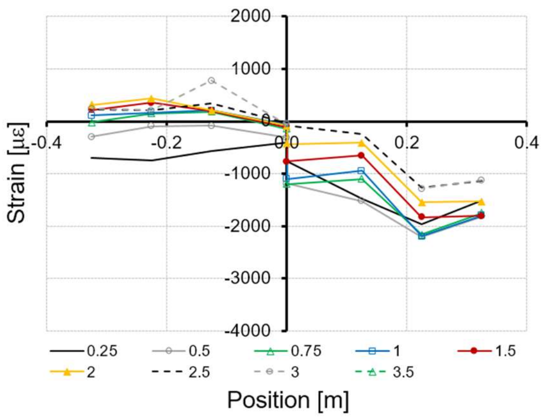

d. A.CA.L1-1. Discontinuous reinforcement. BA4.

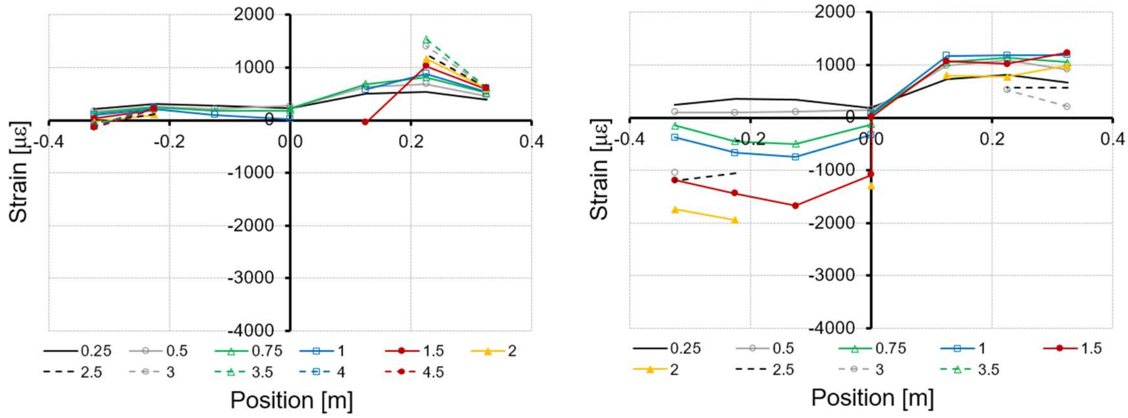

e. A.C.L0. Continuous reinforcement. BA1.

f. A.CA.L1-1. Discontinuous reinforcement. BA1.

Figure 16. Strain for all the drift ratio values in the beam reinforcement of specimens A.C.L0 (left) and A.CA.L1-1 (right). Gravity plus horizontal loads.

Figure 17 gives the unitary column reinforcement strain of specimens *A.C.L0* (without axial load) and *A.C.L1* (with axial load). The *X*-axis represents the distance in metres between the strain gauge and the beam axis. Column reinforcements behaved similarly to the continuous beam reinforcements (Figure 16a), but with some considerable differences:

- Max reinforcement strain took place in the column/beam intersection and continued as far as the beam axis, the point at which tensile strain declined.
- The tensile strain of reinforcement considerably reduced in the sections where column reinforcement was confined by external strengthening.
- The column reinforcement strain substantially reduced when the column was subject to an axial load. The tensile strains at the 1.5% drift ratio were 3,000 με and 900 με for tests *A.C.L0* and *A.C.L1*, respectively.

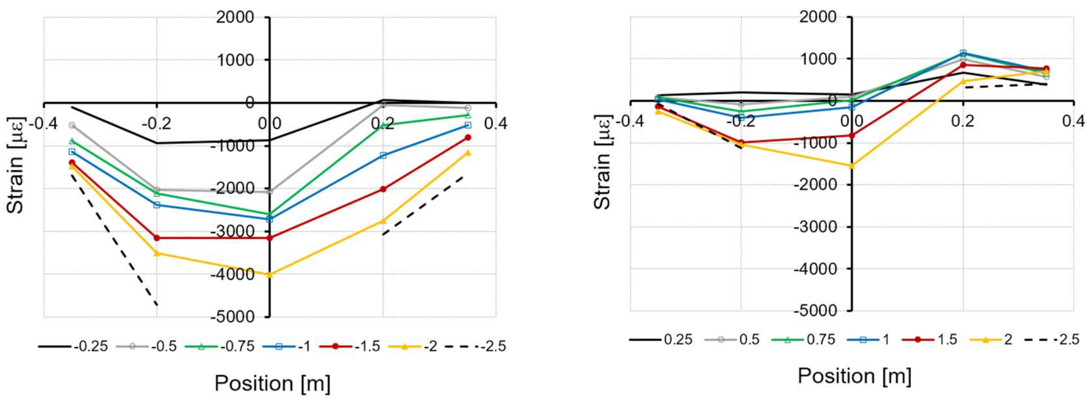

a. Column reinforcement in specimen A.C.L0.

b. Column reinforcement in specimen A.C.L1.

Figure 17. Strain for the drift ratio values in the column reinforcement of specimens A.C.L0 (left) and A.C.L1 (right). Gravity plus horizontal loads.

3.4 Strengthening behaviour

Eight strain gauges were placed on each steel angle (Figure 9), all of which gave similar results due to the symmetry of strengthening and the loads applied to columns (Figure 18). From the figures, we see that:

- The angles on the control specimen (*A.W.L0*) were required to work the least for not having capitals. So the tensile and compression loads that they received were due to friction with the column.
- Capitals allowed compression loads to be transmitted directly between the beam and strengthening (*A.C.L0*).
- The compression strain of angles was the least in the specimen with chemical anchors and capitals with no axial load (*A.CA.L0*). The authors consider that this was due to the degradation of the concrete that came into contact with the capital caused by chemical anchors being pulled out.
- Small tensile strains were measured because angles were not connected to the joint.

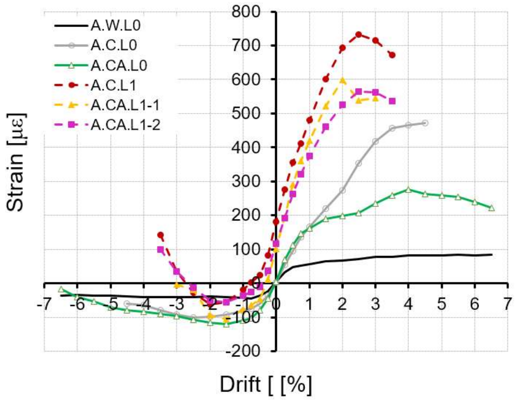

Figure 18. Strain of steel angles.

Figure 19 depicts the participation of strengthening as a mixed section in the column response of three tests (*A.W.L0*, *A.C.L0* and *A.C.L1*). The stress of angles was estimated by multiplying the strain obtained by the modulus of elasticity. This stress was then multiplied by the angle area to obtain force, and the force on each angle was multiplied by the distance to the column axis to obtain the bending moment on the angles in the section where strain gauges were placed (Figure 9).

The left-hand column in Figure 19 gives: the bending moment value in the section with strain gauges (*M.Total*), the bending moment borne by angles (*M.Angles*, estimated from the strain values), the bending moment borne by the reinforced concrete section of the column in this zone (*M.RC*, calculated from the difference between *M.Total* and *M.Angles*). The right-hand column in Figure 19 gives the percentage participation of angles and the reinforced concrete section in relation to the total bending moment of the section under study.

The bending capacity of the reinforced concrete column (*M.MaxRC*) was obtained experimentally from the test run on the control specimen by multiplying the maximum shear load obtained (Figure 10a, Table 2) by the distance to the column/joint intersection, where longitudinal reinforcement yielding occurred. This bending capacity of the reinforced concrete column can be found in Figure 19a and Figure 19b, denoted by a dashed red line.

In the control specimen, the percentage contribution of angles ranged between 21% and 28% (Figure 19a). This was the lowest percentage as the contribution was obtained solely via the contact of materials in a short length (220 mm). Including the capital increased the column's max bending moment, in which angles contributed 38% at the beginning of the test and amounted to 68% when it ended (Figure 19b). In specimen *A.C.L1,* the bending strength was shared almost equally between angles and the reinforced concrete section (Figure 19c).

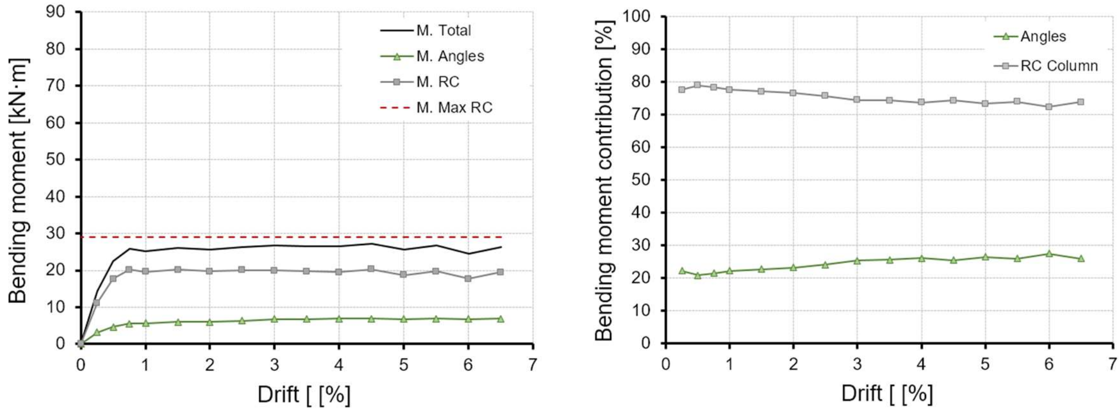

a. A.W.L0

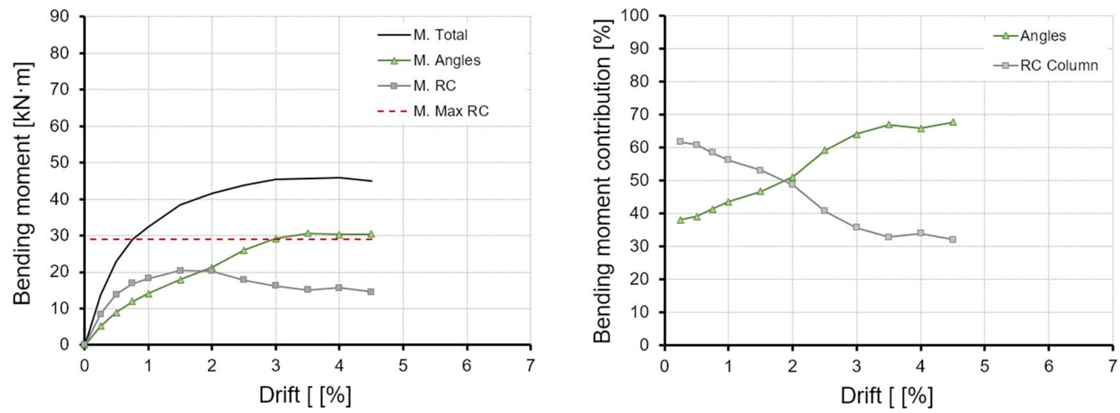

b. A.C.L0

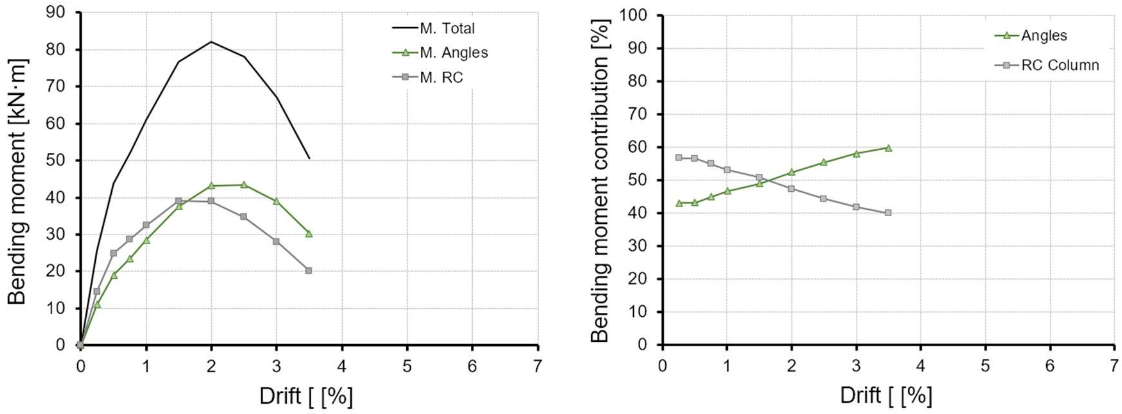

c. A.C.L1

Figure 19. Behaviour of the composite column section subject to the bending moment (A.W.L0, A.C.L0) and flexocompression (A.C.L1). On the left, the bending moment resisted by the reinforced concrete section and angles. On the right, the percentage contribution of both elements to bending moment strength.

4. Conclusions

This paper describes an experimental study run on seven full-scale reinforced concrete beam-column joints with non-ductile details and strengthened externally by steel caging. Beams were reinforced asymmetrically with overlaps inside the joint and designed to resist gravity loads only. An initial gravity load was applied to beams, followed by horizontal cyclic loads. In some specimens, an axial load was applied to the column to study its influence on joint behaviour. All the columns were strengthened externally in the same way by steel angles and battens. Two methods to connect the column jacket to the joint by steel capitals were analysed. The following details of specimens' behaviour were observed:

- The specimen strengthened without capitals was highly ductile and its max bending capacity was limited by the yielding of column reinforcement, which occurred in the column/joint intersection and caused serious cracking.
- Applying the capitals that came into contact with the joint added 65% to the maximum load resisted by the control specimen. Capitals transmitted compression loads directly between the steel caging and joint, and increased the column's mechanical bending arm.
- Using chemical anchors to connect capitals and the joint reduced the response of the specimens with no applied axial load.
- An axial load on the column increased the horizontal load resisted by specimens, although the specimens with axial loads presented more brittle behaviour than the specimens with no axial load.
- The bond between reinforcement and concrete inside the joint was lost after the first cycles. The continuous reinforcement started working as ties between beams through the joint: discontinuous reinforcement became useless under gravity loads.

- Applying an axial load to columns improved both the continuous and discontinuous reinforcement anchorages inside the joint
- The greatest column reinforcement strain took place at the column/joint intersection, although it rapidly declined in the section confined by strengthening. The cases with an applied axial load to the column recorded less column reinforcement strain.
- Angles contributed notably to the bending moments of the mixed steel cage-reinforced concrete section. With steel angles only, the contribution of the strengthening bending moment was around 21-28% in a section close to the joint, where loads were transferred by friction between angles and mortar on the column surface at a distance of only 220 mm. This rose to 68% with the capitals welded to angle ends. In this case, tensile loads continued to be transmitted by friction, but compression loads were also transmitted by the direct contact between the capital and joint.

This study highlights the improvement conferred to the beam-column joint by this type of strengthening and the importance of applying the gravity load to beams to study real joint behaviour and reinforcement anchorage conditions. We observed that by using only steel capitals, the capacity of the beam-joint unit increased by up to 65% and the widespread use of chemical anchors does not provide extra benefits. As applying the proposed technique does not involve opening the joint panel, its application in practical refurbishment cases is quite simple and does not damage the existing structure. Capitals can transmit compression loads between columns through the joint but, as they are not connected to the joint itself, no tensile loads are transmitted between columns.

Acknowledgements

The authors wish to express their gratitude for the financial support provided by the Spanish Ministry of Science and Innovation and the Spanish Ministry of Economy and Competitiveness with Research Projects BIA 2008-06268 and RTI2018-099091-B-C22.

REFERENCES

[1] J. Adam, Global research continues into strengthening structures against earthquakes, Proc. Inst. Civ. Eng. - Civ. Eng. 168 (2015) 148–148. doi:10.1680/cien.2015.168.4.148.

[2] J. Adam, J. Ingham, Editorial, Eng. Fail. Anal. 34 (2013). doi:10.1016/j.engfailanal.2013.07.029.

[3] S. Doocy, A. Daniels, C. Packer, A. Dick, T.D. Kirsch, The Human Impact of Earthquakes: a Historical Review of Events 1980-2009 and Systematic Literature Review, PLoS Curr. (2013).

doi:10.1371/currents.dis.67bd14fe457f1db0b5433a8ee20fb833.

[4] J.G. Ruiz-Pinilla, J.M. Adam, R. Pérez-Cárcel, J. Yuste, J.J. Moragues, Learning from RC building structures damaged by the earthquake in Lorca, Spain, in 2011, Eng. Fail. Anal. 68 (2016) 76–86. doi:10.1016/j.engfailanal.2016.05.013.

[5] O. Murat, Field Reconnaissance of the October 23, 2011, Van, Turkey, Earthquake: Lessons from Structural Damages, J. Perform. Constr. Facil. 29 (2015) 04014125. doi:10.1061/(ASCE)CF.1943-5509.0000532.

[6] E. Baran, H.C. Mertol, B. Gunes, Damage in reinforced-concrete buildings during the 2011 Van, Turkey, earthquakes, J. Perform. Constr. Facil. 28 (2014) 466–479. doi:10.1061/(ASCE)CF.1943-5509.0000396.

[7] M. Tapan, M. Comert, C. Demir, Y. Sayan, K. Orakcal, A. Ilki, Failures of structures during the October 23, 2011 Tabanlı (Van) and November 9, 2011 Edremit (Van) earthquakes in Turkey, Eng. Fail. Anal. 34 (2013) 606–628. doi:10.1016/j.engfailanal.2013.02.013.

[8] S. Ates, V. Kahya, M. Yurdakul, S. Adanur, Damages on reinforced concrete buildings due to consecutive earthquakes in Van, Soil Dyn. Earthq. Eng. 53 (2013) 109–118. doi:10.1016/j.soildyn.2013.06.006.

[9] H. Kaplan, S. Yilmaz, H. Binici, E. Yazar, N. Çetinkaya, May 1, 2003 Turkey—Bingöl earthquake: damage in reinforced concrete structures, Eng. Fail. Anal. 11 (2004) 279–291. doi:10.1016/J.ENGFAILANAL.2003.08.005.

[10] D. Mitchell, R.H. DeVall, K. Kobayashi, R. Tinawi, W.K. Tso, Damage to concrete structures due to the January 17, 1995, Hyogo-ken Nanbu (Kobe) earthquake, Can. J. Civ. Eng. 23 (1996) 757–770. doi:10.1139/l96-886.

[11] N. Augenti, F. Parisi, Learning from Construction Failures due to the 2009 L'Aquila, Italy, Earthquake, J. Perform. Constr. Facil. 24 (2010) 536–555. doi:10.1061/(ASCE)CF.1943-5509.0000122.

[12] M.H. Arslan, H.H. Korkmaz, What is to be learned from damage and failure of reinforced concrete structures during recent earthquakes in Turkey?, Eng. Fail. Anal. 14 (2007) 1–22. doi:10.1016/j.engfailanal.2006.01.003.

[13] D. Bru, A. González, F.J. Baeza, S. Ivorra, Seismic behavior of 1960's RC buildings exposed to marine environment, Eng. Fail. Anal. 90 (2018) 324–340. doi:10.1016/J.ENGFAILANAL.2018.02.011.

[14] S. Yin, Y. Li, S. Li, Y. Yang, Seismic Performance of RC Columns Strengthened with Textile-Reinforced Concrete in Chloride Environment, J. Compos. Constr. 24 (2020) 04019062.

doi:10.1061/(ASCE)CC.1943-5614.0000992.

[15] S. Raza, M.K.I. Khan, S.J. Menegon, H.-H. Tsang, J.L. Wilson, Strengthening and Repair of Reinforced Concrete Columns by Jacketing: State-of-the-Art Review, Sustainability. 11 (2019) 3208. doi:10.3390/su11113208.

[16] J. Ramírez, Ten concrete column repair methods, Constr. Build. Mater. 10 (1996) 195–202. doi:10.1016/0950-0618(95)00087-9.

[17] K.G. Vandoros, S.E. Dritsos, Concrete jacket construction detail effectiveness when strengthening RC columns, Constr. Build. Mater. 22 (2008) 264–276. doi:10.1016/J.CONBUILDMAT.2006.08.019.

[18] S.M. Mourad, M.J. Shannag, Repair and strengthening of reinforced concrete square columns using ferrocement jackets, Cem. Concr. Compos. 34 (2012) 288–294. doi:10.1016/J.CEMCONCOMP.2011.09.010.

[19] A. Napoli, R. Realfonzo, RC Columns Strengthened with Novel CFRP Systems: An Experimental Study, Polymers (Basel). 7 (2015) 2044–2060. doi:10.3390/polym7101499.

[20] M.A.G. Silva, Behavior of square and circular columns strengthened with aramidic or carbon fibers, Constr. Build. Mater. 25 (2011) 3222–3228. doi:10.1016/J.CONBUILDMAT.2011.03.007.

[21] L.P. Ye, K. Zhang, S.H. Zhao, P. Feng, Experimental study on seismic strengthening of RC columns with wrapped CFRP sheets, Constr. Build. Mater. 17 (2003) 499–506. doi:10.1016/S0950-0618(03)00047-3.

[22] P.A. Calderón, J.M. Adam, S. Ivorra, F.J. Pallarés, E. Giménez, Design strength of axially loaded RC columns strengthened by steel caging, Mater. Des. 30 (2009) 4069–4080. doi:10.1016/j.matdes.2009.05.014.

[23] J. Garzón-Roca, J. Ruiz-Pinilla, J.M. Adam, P.A. Calderón, An experimental study on steel-caged RC columns subjected to axial force and bending moment, Eng. Struct. 33 (2011) 580–590. doi:10.1016/j.engstruct.2010.11.016.

[24] L. Cirtek, RC columns strengthened with bandage — experimental programme and design recommendations, Constr. Build. Mater. 15 (2001) 341–349. doi:10.1016/S0950-0618(01)00015-0.

[25] P. Nagaprasad, D.R. Sahoo, D.C. Rai, Seismic strengthening of RC columns using external steel cage, Earthq. Eng. Struct. Dyn. 38 (2009) 1563–1586. doi:10.1002/eqe.917.

[26] M.F. Belal, H.M. Mohamed, S.A. Morad, Behavior of reinforced concrete columns strengthened by steel jacket, HBRC J. 11 (2015) 201–212. doi:10.1016/j.hbrcj.2014.05.002.

[27] T. Chrysanidis, I. Tegos, Axial and transverse strengthening of R/C circular columns: Conventional and new type of steel and hybrid jackets using high-strength mortar, J. Build. Eng. 30 (2020) 101236. doi:10.1016/J.JOBE.2020.101236.

[28] E. Choi, S.H. Park, B.S. Cho, D. Hui, Lateral reinforcement of welded SMA rings for reinforced concrete columns, J. Alloys Compd. 577 (2013). doi:10.1016/j.jallcom.2012.02.135.

[29] H. Naderpour, M. Mirrashid, Classification of failure modes in ductile and non-ductile concrete joints, Eng. Fail. Anal. 103 (2019) 361–375. doi:10.1016/J.ENGFAILANAL.2019.04.047.

[30] D.M. Cotsovos, Cracking of RC beam/column joints: Implications for the analysis of frame-type structures, Eng. Struct. 52 (2013) 131–139. doi:10.1016/J.ENGSTRUCT.2013.02.018.

[31] A. Borghini, F. Gusella, A. Vignoli, Seismic vulnerability of existing R.C. buildings: A simplified numerical model to analyse the influence of the beam-column joints collapse, Eng. Struct. 121 (2016) 19–29. doi:10.1016/J.ENGSTRUCT.2016.04.045.

[32] A. Ghobarah, A. Biddah, Dynamic analysis of reinforced concrete frames including joint shear deformation, Eng. Struct. 21 (1999) 971–987. doi:10.1016/S0141-0296(98)00052-2.

[33] M.H. Harajli, Bond Stress–Slip Model for Steel Bars in Unconfined or Steel, FRC, or FRP Confined Concrete under Cyclic Loading, J. Struct. Eng. 135 (2009) 509–518. doi:10.1061/(ASCE)0733-9445(2009)135:5(509).

[34] L.K.A.Z. M Engindeniz, Repair and strengthening of reinforced concrete beam-column joints: state of the art, ACI Struct J. 102 (2005) 187–197.

[35] A. Pimanmas, P. Chaimahawan, Cyclic Shear Resistance of Expanded Beam-Column Joint, Procedia Eng. 14 (2011) 1292–1299. doi:10.1016/J.PROENG.2011.07.162.

[36] E.S. Lam, B. Li, Z. Xue, K. Leung, J.Y. Lam, Experimental studies on reinforced concrete interior beam-column joints strengthened by unsymmetrical chamfers, Eng. Struct. 191 (2019) 575–582. doi:10.1016/J.ENGSTRUCT.2019.03.099.

[37] R. Realfonzo, A. Napoli, J.G.R. Pinilla, Cyclic behavior of RC beam-column joints strengthened with FRP systems, Constr. Build. Mater. 54 (2014) 282–297. doi:10.1016/j.conbuildmat.2013.12.043.

[38] A. Prota, A. Nanni, G. Manfredi, E. Cosenza, Selective upgrade of underdesigned reinforced beam-column joints using carbon fiber-reinforced concrete, ACI Struct. J. 101 (2004) 699–707.

[39] C. Del Vecchio, M. Di Ludovico, A. Balsamo, A. Prota, G. Manfredi, M.

Dolce, Experimental Investigation of Exterior RC Beam-Column Joints Retrofitted with FRP Systems, J. Compos. Constr. 18 (2014) 04014002. doi:10.1061/(ASCE)CC.1943-5614.0000459.

[40] Y.T. Obaidat, G.A.F.R. Abu-Farsakh, A.M. Ashteyat, Retrofitting of partially damaged reinforced concrete beam-column joints using various plate-configurations of CFRP under cyclic loading, Constr. Build. Mater. 198 (2019) 313–322. doi:10.1016/J.CONBUILDMAT.2018.11.267.

[41] S. Sasmal, K. Ramanjaneyulu, B. Novák, V. Srinivas, K. Saravana Kumar, C. Korkowski, C. Roehm, N. Lakshmanan, N.R. Iyer, Seismic retrofitting of nonductile beam-column sub-assemblage using FRP wrapping and steel plate jacketing, Constr. Build. Mater. 25 (2011) 175–182. doi:10.1016/J.CONBUILDMAT.2010.06.041.

[42] M. Kazem Sharbatdar, A. Kheyroddin, E. Emami, Cyclic performance of retrofitted reinforced concrete beam–column joints using steel prop, Constr. Build. Mater. 36 (2012) 287–294. doi:10.1016/J.CONBUILDMAT.2012.04.115.

[43] J. Shafaei, A. Hosseini, M.S. Marefat, Seismic retrofit of external RC beam–column joints by joint enlargement using prestressed steel angles, Eng. Struct. 81 (2014) 265–288. doi:10.1016/J.ENGSTRUCT.2014.10.006.

[44] G. Campione, L. Cavaleri, M. Papia, Flexural response of external R.C. beam–column joints externally strengthened with steel cages, Eng. Struct. 104 (2015) 51–64. doi:10.1016/J.ENGSTRUCT.2015.09.009.

[45] W.T. Lee, Y.J. Chiou, M.H. Shih, Reinforced concrete beam-column joint strengthened with carbon fiber reinforced polymer, Compos. Struct. 92 (2010) 48–60. doi:10.1016/j.compstruct.2009.06.011.

[46] B. Li, T.-C. Pan, C.T.N. Tran, Effects of axial compression load and eccentricity on seismic behavior of nonseismically detailed interior beam-wide column joints, J. Struct. Eng. 135 (2009) 774–784. doi:10.1061/(ASCE)0733-9445(2009)135:7(774).

[47] R.P. Dhakal, T.-C. Pan, P. Irawan, K.-C. Tsai, K.-C. Lin, C.-H. Chen, Experimental study on the dynamic response of gravity-designed reinforced concrete connections, Eng. Struct. 27 (2005) 75–87. doi:10.1016/j.engstruct.2004.09.004.

[48] C.P. Pantelides, Y. Okahashi, L.D. Reaveley, Seismic rehabilitation of reinforced concrete frame interior beam-column joints with FRP composites, J. Compos. Constr. 12 (2008) 435–445. doi:10.1061/(ASCE)1090-0268(2008)12:4(435).

[49] E. Giménez, J.M. Adam, S. Ivorra, P.A. Calderón, Influence of strips configuration on the behaviour of axially loaded RC columns strengthened by steel angles and strips, Mater. Des. 30 (2009) 4103–

4111. doi:10.1016/j.matdes.2009.05.010.

[50] J. Garzón-Roca, J. Ruiz-Pinilla, J.M. Adam, P.A. Calderón, An experimental study on steel-caged RC columns subjected to axial force and bending moment, Eng. Struct. 33 (2011) 580–590. doi:10.1016/j.engstruct.2010.11.016.

[51] J.M. Adam, S. Ivorra, F.J. Pallarés, E. Giménez, P.A. Calderón, Axially loaded RC columns strengthened by steel caging. Finite element modelling, Constr. Build. Mater. 23 (2009) 2265–2276. doi:10.1016/J.CONBUILDMAT.2008.11.014.

[52] A. Beres, S.P. Pessiki, R.N. White, P. Gergely, Implications of experiments on the seismic behavior of gravity load designed RC beam-to-column connections, Earthq. Spectra. 12 (1996) 185–198. doi:10.1193/1.1585876.

[53] S. Hakuto, R. Park, H. Tanaka, Seismic load tests on interior and exterior beam-column joints with substandard reinforcing details, ACI Struct. J. 97 (2000) 11–25.

[54] H. Yang, W. Zhao, Z. Zhu, J. Fu, Seismic behavior comparison of reinforced concrete interior beam-column joints based on different loading methods, Eng. Struct. 166 (2018) 31–45. doi:10.1016/J.ENGSTRUCT.2018.03.022.

[55] W.T. Lee, Y.J. Chiou, M.H. Shih, Reinforced concrete beam–column joint strengthened with carbon fiber reinforced polymer, Compos. Struct. 92 (2010) 48–60. doi:10.1016/J.COMPSTRUCT.2009.06.011.

[56] B. Li, H.Y.G. Chua, Seismic performance of strengthened reinforced concrete beam-column joints using FRP composites, J. Struct. Eng. 135 (2009) 1177–1190. doi:10.1061/(ASCE)0733-9445(2009)135:10(1177).

[57] J.-Y. Lee, J.-Y. Kim, G.-J. Oh, Strength deterioration of reinforced concrete beam–column joints subjected to cyclic loading, Eng. Struct. 31 (2009) 2070–2085. doi:10.1016/J.ENGSTRUCT.2009.03.009.

[58] F.T.K. Au, K. Huang, H.J. Pam, Diagonally-reinforced beam–column joints reinforced under cyclic loading, Proc. Inst. Civ. Eng. - Struct. Build. 158 (2005) 21–40. doi:10.1680/stbu.2005.158.1.21.

[59] S. Alavi-Dehkordi, D. Mostofinejad, P. Alaee, Effects of high-strength reinforcing bars and concrete on seismic behavior of RC beam-column joints, Eng. Struct. 183 (2019) 702–719. doi:10.1016/J.ENGSTRUCT.2019.01.019.